Effects of Nonrigid Registrations on DBM Analysis Using SSD Model

Z. Han[1,2], X. Yang[1], B. A. Landman[1,2], J. C. Gore[2], and B. M. Dawant[1]

[1]Electrical Engineering, Vanderbilt University, Nashville, TN, United States, [2]Institute of Imaging Science, Vanderbilt University, Nashville, TN, United States

Introduction

Deformation Based Morphometry (DBM) aims to detect morphological differences between groups based on statistical analysis of deformation fields generated by non-rigid registrations, which warp individual volumes to a standard coordinate system [1]. Since DBM relies on the deformation fields obtained from non-rigid registrations, it is very important to assess and compare the effect of various registration techniques on the performance of DBM analysis. Several studies have compared non-rigid registration algorithms [2-3]. Most notably, Klein et al [3] conducted a comprehensive evaluation of 14 nonlinear deformation algorithms by comparing atlas-based segmentation with manual tracing. However, few studies have compared the effect of registration algorithms on population differences that may be uncovered through DBM, presumably due to a lack of “ground truth” for deformation fields. In this study, we simulated two groups of normal brain images and deformation fields via the Statistical Simulation of Deformations (SSD) model [4], introduced known growths in one group, and evaluated the effect of five different nonrigid registration methods on DBM analysis of the groups without and with growths.

Methods

Thirty-six MRI brain images obtained from normal children (20 males and 16 females, 8.9±0.4 years old) were used in this study to produce deformation fields to train the SSD model. Preprocessing steps included bias field correction and skull stripping, followed by an affine alignment to one volume in the dataset (henceforth referred to as the atlas). The five non-rigid registration algorithms used in this study are: (1) Adaptive Basis Algorithm (ABA) [5]; (2) Image Registration Toolkit (IRTK) [6]; (3) FSL Nonlinear Image Registration Tool (FSL) [7]; (4) Automatic Registration Tools (ART) [8]; and (5) The standard normalization utility available in SPM8 [9]. To reduce the bias towards one particular registration method, the remaining thirty-five subjects in the dataset were randomly assigned into five groups of seven subjects, with each group adopting one registration method. The SSD model was then trained with the set of all the deformation fields generated, and was finally sampled randomly to produce two groups of twenty simulated MRI images (called G1 and G2) and associated deformation fields. A growth model with known sizes and locations was subsequently applied to the G2 group to simulate pathologies (noted as GG2). To evaluate the effect of non-rigid registration algorithms, the five methods listed above were used to warp each volume in the G1 group and GG2 group to the atlas, yielding five deformation fields for each subject. From each of the deformation fields, Jacobian was calculated voxel-wise to characterize local tissue compression or expansion. Group mean Jacobian maps were obtained and color-coded for each of the five methods for visual inspection. To statistically quantify the effect of registration, a General Linear Model in SPM8 [9] was implemented on the Jacobian maps voxel-wise between the G1 and GG2 groups for each method (thresholded at uncorrected p<=0.001 and FWE corrected p<=0.05). The ground truth Jacobians from the growth model were used as the basis of comparisons.

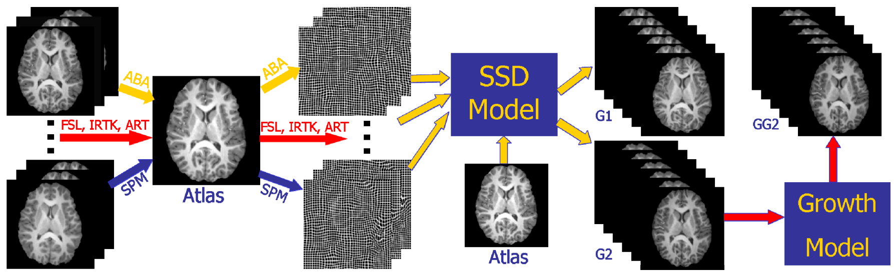

Fig.1. SSD model training and the simulation process to obtain the images in G1 and GG2 groups.

Results

Figure 1 shows a flowchart for the SSD model training with the set of 35 deformation fields generated from five registration methods, and the simulation process to obtain the MRI images in G1 and GG2 groups. The color-coded group mean Jacobian for G1 (top row) and GG2 (bottom row) based on five methods is shown in Figure 2. Warm colors denote volume increases, cold colors denote volume decreases, and the green color indicates no volume changes. As can be seen, the ABA and ART yield more localized Jacobian maps, while maps from the IRTK and FSL are smoother and more similar with each other. The SPM Jacobian maps for both the groups are over smooth so that local deformation details are virtually invisible. This could arise from a low degree of deformation in the normalization utility in the SPM8. Figure 3 shows the statistical results of T maps for Jacobian differences between the G1 and GG2 groups based on each method, thresholded at uncorrected p <= 0.001 (T>=3.319) and overlaid on the atlas. The ABA, IRTK, FSL, and ART showed clusters of statistically significance after multiple comparison correction with FWE, whereas the DBM based on SPM normalization failed to locate any clusters with the same statistical criteria. As a reference, the “ground truth” Jacobian map (>1) in the growth model is shown on the right most in Figure 3.

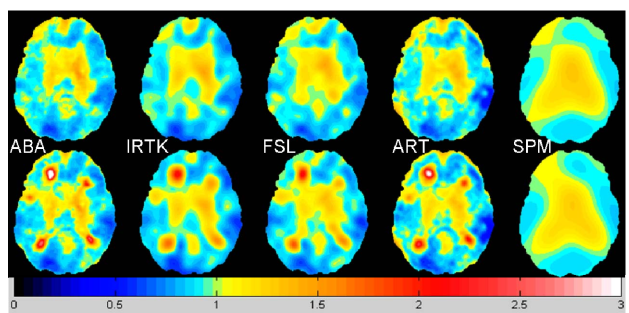

Fig.2. Color-coded group mean Jacobian maps for G1 (top) and G2 (bottom). Warm/cold colors mean the volume increase/decrease.

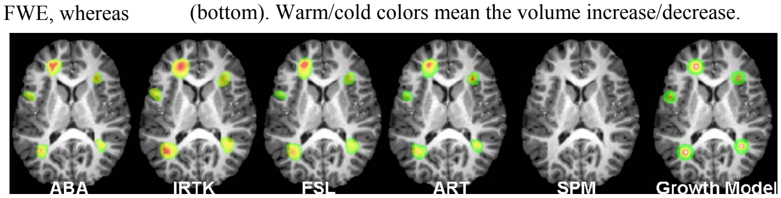

Fig.3. DBM results of T maps thresholded at uncorrected p<=0.001 (T >= 3.319) overlaid on the atlas by five methods. The right image is the Jacobian (>1) in the growth model.

Conclusion

This preliminary study shows that different registration methods may perform differently on the statistical group comparisons of Jacobian values in DBM. ABA and ART are less smooth than IRTK and FSL. More experiments on the effect of different parameters, e.g. growth sizes and noise levels, are on-going to quantify the sensitivity and specificity of each algorithm. We are building a fully automatic pipeline to systematically evaluate different parameters in the growth model and the SSD model.

Acknowledgement

The authors would like to thank ACCRE for the parallel computing. The study was supported by the U.S. Department of Commerce grant BS123456, the NICHD grants R0135681-06 and P30HD15052-24, the NIH Roadmap for Medical Research Grant T32MH075883.

References

[1] Ashburner J, *et.al*. Hum Brain Mapp,1998, 6(5): 348-57. [2] www.nirep.org [3] Klein, A. *et.al.* NeuroImage, 2009, 46(3) :786-802. [4] Xue Z. *et.al.*NeuroImage, 2006, 33(3) :855-66. [5] Rohde GK, *et.al.* IEEE TMI, 2003, 22(11): 1470-9. [6] Rueckert, D. *et.al.* IEEE TMI, 1999, 18(8): 712-21. [7] www.fmrib.ox.ac.uk/fsl/fnirt/ [8] Ardekani, B. *et.al.* J.Neurosci Methods, 2005, 142(1) : 67-76. [9] www.fil.ion.ucl.ac.uk/spm/.